



Fatigue behavior prediction of welded joints by using an integrated fracture mechanics approach

Mirco D. Chapetti*, Leandro F. Jaureguizar

Laboratory of Experimental Mechanics (LABMEX), INTEMA (Research Institute for Materials Science and Technology), CONICET – National University of Mar del Plata, Juan B. Justo 4302 (B7608FDQ) Mar del Plata, Argentina

ARTICLE INFO

Article history:

Received 2 October 2011
Received in revised form 30 January 2012
Accepted 3 February 2012
Available online 22 February 2012

Keywords:

Welded joints
Fatigue
Fracture mechanics
Short cracks
Long cracks

ABSTRACT

Current fracture mechanics methods for fatigue assessment of welded joints are based on long crack behavior. The present work introduces a method to predict the fatigue strength of welded joints by means of an integrated fracture mechanics approach (IFMA) that takes into account the fatigue behavior of short cracks. This methodology estimates the fatigue crack propagation rate as a function of the difference between the applied driving force and the material threshold for crack propagation, function of crack length. Firstly, the proposed fracture mechanic method is introduced and compared with the traditional fracture mechanic approach, used mainly for fitness for purpose assessment of welded joints with cracks or other crack-like defects. Then, the method is used for several theoretical and parametric applications to show its ability to predict the influence of different mechanical, geometrical and microstructural parameters in the definition of the fatigue resistance of welded joints. The influence of plate thickness, initial crack length and reinforcement angle on fatigue strength of butt-welded joints has been analysed and results show good agreement with experimental trends. Finally, the method is applied to predict and analyze the fatigue behavior of butt welded and non-load-carrying transverse fillet welded joints, and estimated and experimental results are analysed and compared.

© 2012 Elsevier Ltd. All rights reserved.

1. Introduction

Welds are often the weakest portions of structures and the related welding process has significant influence on the integrity of structures. Welding defects that may be introduced during fabrication are only generally considered in commonly applied fatigue design rules for welded structures that are based primarily on $\Delta\sigma_n$ - N curves [1]. However, advances in welding material and technology allows an easy control of weld geometry such as weld profile, throat thickness and flank angle. Fabricators are willing to invest in welds with consistently higher fatigue strength, thus it is important to produce welds with known and adequate fatigue design strength at a reasonable cost. To do so, a better understanding of the fatigue behavior of welded joints with consideration of all the involved factors is necessary. So, it is important to quantify the link between weld geometry, defects, material properties and fatigue strength. Besides, a model or approach capable of doing that could help to understand how the fatigue resistance of a given joint is defined and how it can be improved.

It is well known that in many technical fields the concept of nominal stress still prevails in the design of welded joints and its

application requires the definition of the nominal stress and its permissible value with reference to a corresponding classified structural detail. In the design code for welded joints (for instance, the IIW recommendations [1]), the fatigue design categories of welded structural details are abbreviated by FAT (fatigue design class) combined with a number that designates the allowable nominal stress range $\Delta\sigma_n$ (MPa) at $N = 2 \times 10^6$ cycles with the survival probability $P_s = 97.7\%$. The fatigue design curves are valid for any R ratio and for a given material (steel or aluminum).

However, in case of more complex structural details, to which neither a nominal stress nor a design category can be assigned; only local concepts are applicable [1–4]. The fatigue process has a local character and cannot be well described by nominal stresses. Some more recently special variants of the local concepts are proposed; however, these are under controversial discussion at the time being, and the presented concept variants and related issues are arbitrary to some extent. Thus the basic physical facts behind these methods should be properly considered. The technical crack initiation phase should also be further subdivided into an initiation life at the microstructure scale and a short-crack propagation life, but this is not yet under discussion in the local concepts of fatigue assessment of welded joints.

Another aspect that should be taken into consideration is that the existence of crack-like imperfections in welded joints is normally assumed to eliminate the crack initiation stage of fatigue life.

* Corresponding author.

E-mail address: mchapetti@fi.mdp.edu.ar (M.D. Chapetti).

Nomenclature

a	crack length	ΔK_{dR}	microstructural threshold
a_i	initial crack length	ΔK_{th}	fatigue crack propagation threshold
a_f	final crack length	ΔK_{thR}	fatigue crack propagation threshold for long cracks
A	constant of Woehler $\Delta\sigma_n$ - N curve	h	weld reinforcement height
α	weld reinforcement angle	k	material constant that takes into account the development of ΔK_C
C and m	environmentally sensitive material-constants	k_{tx}	stress concentration at a given distance x from the weld toe surface
c	half surface crack length	M_k	correction factor
d	microstructural dimension (e.g. grain size)	N	total fatigue life
da/dN	crack propagation rate	N_f	fatigue crack initiation life
$\Delta\sigma_e$	fatigue limit (endurance: 10^7 cycles)	N_p	fatigue crack propagation life
$\Delta\sigma_{eR}$	smooth fatigue limit	R	stress ratio (minimum stress/maximum stress)
$\Delta\sigma_n$	nominal applied stress range	ρ	weld toe radius
$\Delta\sigma_{th}$	threshold stress range for crack propagation	t	plate thickness
$\Delta\sigma_{yy}(x)$	local applied stress range	t_0	reference plate thickness
$\Delta\sigma_t$	welded joint fatigue limit for the thickness t	w	weld reinforcement width
$\Delta\sigma_{t0}$	welded joint fatigue limit for the reference thickness t_0	x	distance from the weld toe surface along the crack path
ΔK	applied stress intensity factor range	Y	crack shape parameter
ΔK_C	extrinsic component of ΔK_{th}		
ΔK_{CR}	extrinsic component of ΔK_{thR}		

Because small, sharp, slag intrusions are unavoidably present at the weld toe and act as crack initiation sites, the fatigue life of a welded joint is predominantly controlled by the crack propagation process [5]. Metallurgical examinations show that the average depth of these flaws is 0.15 mm and typically the maximum depth is approximately 0.4 mm [6,7]. A review by Grover [8] suggested that even high-quality welds contain flaws up to a depth of about 0.1 mm. Other previous works on fatigue of welded joint have observed initial crack-like defect depths of about 10–120 μm [9], 20–150 μm [10] or 10–400 μm [11], according to the welding conditions and applied quality control. Radaj and Sonsino have recommended initial crack size $a_i = 0.1$ –0.25 mm in welded structures for life predictions [2]. These defect depths clearly fall on the short crack regime, thus the short crack behavior should be taken into account in any analysis in which the initial crack length is within the range of 20–400 μm . Verreman and Nie [12] found that micro-crack initiation is a small fraction of the total fatigue life (an average of 6%), and that the life cycles needed to create a crack with 0.5 mm in length is 25–50% of the total fatigue life and can be termed as “short-crack propagation life”. If the total fatigue life of a weld detail is estimated as the number of cycles to propagate a long crack (e.g. 0.5 mm) till fracture, the estimation will surely be conservative in those details where the initial crack length is about 0.1–0.2 mm and a short crack propagation life should be added to the result. So instead of dealing with crack initiation life, almost un-predictable in the case of welded details, it would be possible to get better estimations by including the short crack propagation period in the crack propagation life estimation.

Therefore, the emphasis of the fatigue assessment for most welded structures should be focused on the crack growth portion of fatigue life, which can be assessed by using the linear elastic fracture mechanics. By characterizing stable crack growth using the stress intensity factor range ΔK , the crack growth rate of a weld during cyclic loading can be predicted, and hence the number of cycles necessary for a crack to extend from some initial size, i.e. the size of pre-existing crack or crack-like defects, to a maximum permissible size to avoid catastrophic failures. However, this approach is usually applied by using a simple fatigue crack propagation Paris law that does not take into account the threshold for fatigue crack propagation. Besides, the short crack effect on that threshold is not taken into consideration. One of the main consequences of this procedure is that the fatigue threshold associated to a given weld profile cannot be defined or estimated.

In this work an integrated fracture mechanics approach is proposed and used to predict the fatigue behavior of welded joints. Firstly, the proposed fracture mechanic method is introduced and compared with the traditional fracture mechanic approach used mainly for fitness for purpose assessment of welded joints with cracks or other crack-like defects. Then the method is used for several theoretical and parametric applications to show its ability to predict the influence of different mechanical, geometrical and microstructural parameters in the definition of the fatigue resistance of welded joints. Finally, the method is applied to predict and analyze the fatigue behavior of butt welded and non-load-carrying transverse fillet welded joints, and the estimated and experimental results are compared.

2. The traditional fracture mechanics approach applied to welded joints

In the traditional application the fracture mechanic approach is used for damage tolerance analysis. It is usually stated that the fatigue life in numbers of load cycles consists on the initiation life of a technical crack of about 1 mm in depth and the subsequent long-crack propagation life up to final fracture. The approach does not consider that the technical crack initiation life comprises the microstructural crack initiation life and the short-crack propagation life up to that technical crack size. These basic physical facts are not properly considered in the conventional global and more recent local fatigue assessment methods for welded joints. When this traditional approach is applied, the $\Delta\sigma_n$ - N curve is calculated by integrating the Paris–Erdogan crack-growth law [13]:

$$\frac{da}{dN} = C\Delta K^m \quad (1)$$

where m and C are environmentally sensitive material-constants obtained from long crack fatigue behavior, and the stress intensity factor range ΔK is given by the following general expression [13]:

$$\Delta K = Y M_k \Delta\sigma_n \sqrt{\pi a} \quad (2)$$

where Y is a function of crack size and shape ($a/2c$) and of loading, $\Delta\sigma_n$ is the nominal applied stress range, a is the crack length, and M_k is a magnification factor that reflects the stress concentration effect of the welded joint geometry and depends on the crack size, section thickness and loading mode. M_k quantifies the change in

stress intensity factor K as a result of the surface discontinuity at the weld toe.

From (1) and (2), and integrating from an initial crack length (a_i) to a final crack depth (a_f) the resulting $\Delta\sigma_n$ - N curve for a given stress ratio (R) is predicted to be:

$$\Delta\sigma_n^m N = A \quad (3)$$

where A is a constant and N is the number of cycles (fatigue life). According to this expression, the $\Delta\sigma_n$ - N curve is linear on a log-log basis with a slope m equal to that of the Paris law. As a consequence of this, most design $\Delta\sigma_n$ - N curves for welded joints are taken to be parallel with a slope compatible with the fatigue crack law for the material. Since m is approximately 3 for most materials, $\Delta\sigma_n$ - N curves with slopes of 3 are widely adopted [15–17], as recommended for steels in BS 7910 [18] and consistent with the slope of the $\Delta\sigma_n$ - N curve for the as-welded joint. The crack growth parameter C in Eq. (1) can be estimated from experimental results using the initial crack length (when the crack is first observed), the final crack length (for instance, half the plate thickness), the correlation between the crack aspect ratio and crack length, the loading history applied during growth between the initial and final crack lengths, and the M_k solution for the studied weld.

An effect of stress ratio R (minimum to maximum applied stress) is evident at growth rates less than 5×10^{-6} mm/cycle [19]. Below this propagation rate the material exhibits a deviation from the Paris relationship (Expression (3)) used by others [20–22] to describe crack growth in welds. Thus a simple linear relationship between stress intensity and growth rates on logarithmic scales is only accurate when the joints are subjected to high stress ratio or high nominal loads producing crack growth rates faster than 10^{-5} mm/cycle.

Eq. (1) is also recommended by the International Institute of Welding (IIW) [1] to calculate the fatigue crack propagation rate of welded joints made of steel or aluminum. The constants $m = 3$ and $C = 5.21 \times 10^{-13}$ (da/dN in mm/cycle and ΔK in $\text{Nmm}^{3/2}$) are recommended by IIW [1] for the assessment of ferrite–pearlite steel welded joints in the as-welded condition, and $C_{mean} = 1.7 \times 10^{-13}$ [1,23] is usually used, considered as the mean fatigue crack growth rate coefficient. Using the values m and C the cyclic life corresponding to any stress range can be evaluated. The theoretical FAT can then be determined by adjusting the result according to the $\Delta\sigma_n$ - N curve, Eq. (3), so as to give the stress range that corresponds to the fatigue life of two million cycles.

Recently, a threshold value of the stress intensity factor was included in the IIW recommendations [1]. A simple alternative to the linear relationship given by Expression (3) can be then, among others, the following [13,24]:

$$\frac{da}{dN} = C(\Delta K^m - \Delta K_{thR}^m) \quad (4)$$

where ΔK_{thR} is the threshold for long crack growth (a constant value for a given stress ratio), and represents the resistance of the material to fatigue crack propagation. However, this approach cannot deal with short cracks for which the threshold for fatigue crack propagation depends on the crack length, and so the threshold associated to the fatigue limit of a given configuration that is usually related with short cracks or crack-like defects cannot be estimated or analyzed.

3. The proposed fracture mechanics approach

An important factor that is not considered in traditional fracture mechanics approaches is that short cracks usually show lower threshold levels and higher propagation rates than long cracks when the same applied driving force ΔK is considered, and that their threshold for fatigue crack propagation depends of crack

length [25–30]. The short crack effect can be observed until a crack length that depends on the effective stress ratio, R , and can be in the range of 0.5–1 mm for structural steels. In this range of crack the crack closure and other short crack effects are not fully developed, so that the threshold for fatigue crack propagation is lower than that corresponding to long cracks for the same load ratio R .

It is worth noting that each point in the $\Delta\sigma_n$ - N plot corresponds to the fracture of a given specimen and that the total fracture process due to pure fatigue can be divided in five well-defined steps [26,27,31]. Fig. 1 shows schematically the fatigue crack initiation process from surface for a plain specimen. At first, there is the damage accumulation, then the microcrack initiation, the early microcrack propagation that gives rise to a macrocrack formation, and the propagation of this engineering crack to get a fracture. In the traditional fracture mechanics approach the first three steps are usually considered as the crack initiation period (macrocrack initiation).

In the case of fatigue crack initiation from surface, the well-known Kitagawa and Takahashi diagram, also shown in Fig. 1, could be used to deal with the fatigue crack propagation threshold as a function of crack length [32–35]. Different models and theories allow us to handle cracks longer than a microstructural dimension (for instance a grain size d , see Fig. 1) [32–34]. Thus, the pure fatigue crack initiation process can be defined as the number of cycles necessary to give rise to a crack similar in length to the microstructural characteristic dimension, d . The crack propagation stage can then be analyzed from that crack length d .

The proposed fracture mechanics approach to analyze fatigue behavior of welded joints includes the fatigue crack propagation threshold for both short and long cracks ($a \geq d$). The methodology [31], previously developed to analyze the short crack behavior in mechanical components, estimates the threshold for fatigue crack propagation as a function of crack length, ΔK_{th} , and the fatigue crack propagation rate as the difference between the applied driving force, ΔK , and ΔK_{th} , as follow:

$$\frac{da}{dN} = C(\Delta K^m - \Delta K_{th}^m) \quad (5)$$

In Expression (4) the threshold for crack propagation is constant for a given R , but in Expression (5) it is also a function of crack length, then the short crack regime can be properly accounted.

Expression (5) states that the difference between the total applied driving force defined by the applied stress intensity factor range for a given geometrical and loading configuration, ΔK , and the threshold for crack propagation, ΔK_{th} , defines the effective driving force applied to the crack. This concept is the base of the Resistance–Curve Method [32,34]. If the short crack effect is contemplated, according to Fig. 1 the variation of the propagation threshold should be known as a function of crack length. In a previous study [31] an expression to estimate the threshold for fatigue crack propagation as a function of crack length was obtained by using only the plain fatigue limit, $\Delta\sigma_{eR}$, the threshold for long crack, ΔK_{thR} , and the microstructural characteristics dimension, d (e.g. grain size). The expression was defined from a depth given by the position d of the strongest microstructural barrier that defines the smooth fatigue limit (e.g. first grain boundary). A microstructural threshold for crack propagation, ΔK_{dR} , is defined by the plain fatigue limit $\Delta\sigma_{eR}$ and the position d of the strongest microstructural barrier (see Figs. 1 and 2). A total extrinsic threshold to crack propagation, ΔK_{CR} , is then defined by the difference between the crack propagation threshold for long cracks, ΔK_{thR} , and the microstructural threshold, ΔK_{dR} . The development of the extrinsic component is considered to be exponential and a development parameter k is estimated as a function of the same microstructural and mechanical parameter used to define the material threshold

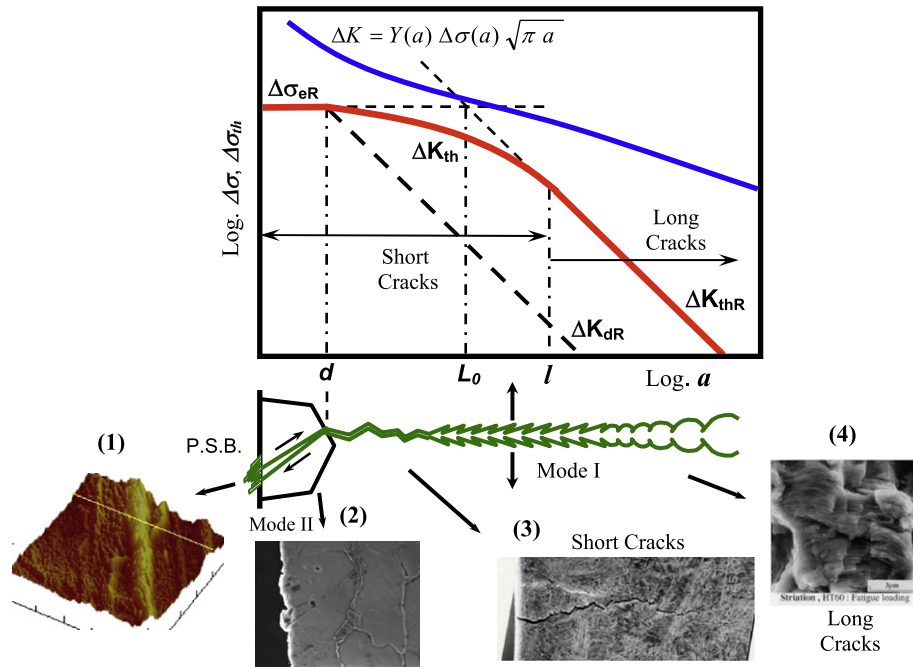


Fig. 1. Mechanical fatigue of materials without cracks or crack-like defects: (1) initial cyclic damage in the form of cyclic hardening or softening, e.g. Persistent Slip Bands, (2) microcrack initiation, (3) microcrack propagation to give rise to an initial engineering-sized flaw (0.5–1 mm), and subsequent macroscopic propagation (4) until final failure or instability (5).

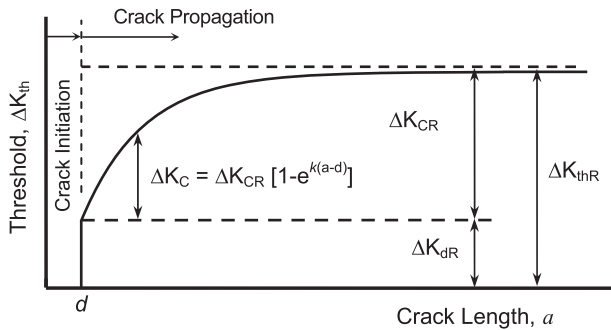


Fig. 2. Threshold curve defined by Expression (6) in terms of the stress intensity factor range.

for crack propagation. The material threshold for crack propagation as a function of the crack length, ΔK_{th} , is then defined as [31]:

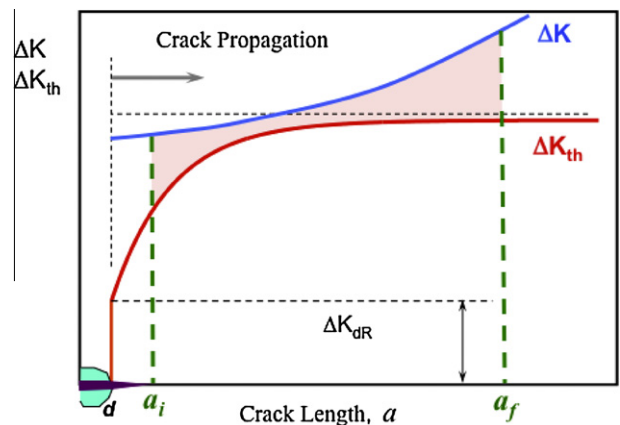
$$\Delta K_{th} = \Delta K_{dR} + (\Delta K_{thR} - \Delta K_{dR}) [1 - e^{-k(a-d)}] = Y \Delta \sigma_{th} \sqrt{\pi a} \quad a \geq d \quad (6)$$

where ΔK_{dR} and k are given by:

$$\Delta K_{dR} = Y \Delta \sigma_{eR} \sqrt{\pi d} \quad (7)$$

$$k = \frac{1}{4d} \frac{\Delta K_{dR}}{(\Delta K_{thR} - \Delta K_{dR})} \quad (8)$$

Fig. 2 shows schematically the threshold curve given by Expression (6) in terms of the stress intensity factor range. For a crack length $a = d$, $\Delta K_{th} = \Delta K_{dR}$, and ΔK_{th} tends to ΔK_{thR} for long cracks. The expression defined to estimate the material threshold for crack propagation as a function of the crack length allows definition of a crack initiation period as the number of load cycles necessary to initiate a crack of depth d (micro-crack initiation), from which the crack propagation behavior can be analyzed. This applies to materials free of crack or crack-like defects. In the case of a welded



Fatigue crack propagation N_p Integration between a_i and a_f

$$\frac{da}{dN} = C \left(\Delta K^m - \Delta K_{th}^m \right)$$

Threshold = $f(Y, \Delta \sigma_{eR}, \Delta K_{thR}, d, R, a)$

Applied $\Delta K = f(Y, M_k, \Delta \sigma_n, a)$

Fig. 3. Schematically explanation of the resistance curve concept and the fatigue life estimation for a given configuration.

joint the presence of defects usually minimizes the crack initiation period, and the initial crack length for the crack propagation period will be given by the maximum crack-like defect.

Fig. 3 shows schematically the concept of the approach given by Expressions (5) and (6). The difference between the total applied driving force defined by the applied stress intensity factor range for a given geometrical and loading configuration, ΔK , and the threshold for crack propagation, ΔK_{th} , defines the effective driving force applied to the crack. Both parameters should be known as a function of crack length. By integrating Expression (5) from an initial crack length (a_i) given by the maximum crack-like defect to a final crack length (a_f) the resulting number of cycles to failure for a given nominal stress $\Delta \sigma_n$ can be estimated. The $\Delta \sigma_n - N$ curve

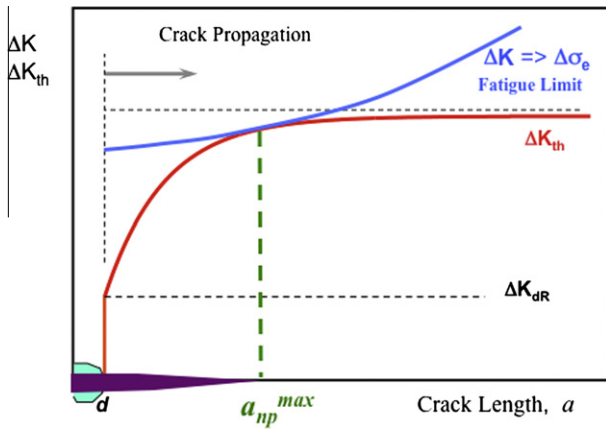


Fig. 4. Schematic explanation of the condition for the threshold associated to the fatigue limit of a given joint configuration.

for a given weld configuration can be then estimated by using Expression (5) and accounting for the short crack effects.

The fatigue limit for a given weld configuration and the associated non-propagation crack can then be easily estimated without knowing the fatigue crack propagation data (C and m). Fig. 4 shows schematically the situation associated to the threshold condition. The value of ΔK should be greater than ΔK_{th} for any crack length (between a_0 and a_f). The fatigue limit $\Delta\sigma_e$ will be given by the nominal stress $\Delta\sigma_n$ for which the applied ΔK becomes equal to ΔK_{th} for a given crack length (see Fig. 4). Then the tangent condition defines the associated non-propagating crack length associated to the joint configuration. The maximum defect size allowable for that configuration can also be known, so that the approach can also analyze the defect size sensitivity of the configuration.

4. Some theoretical and parametric applications

The influence of parameters like plate thickness, initial crack length and reinforcement angle on fatigue strength of butt-welded joints has been theoretically analyzed in a previous publication [36], and results have shown good agreement with experimental results and trends. Below there is a brief description of an example of those previous analyses which clearly show the ability of the approach to account for the influence of different geometrical, mechanical and microstructural parameters associated with the joint configuration.

4.1. Influence of reinforcement angle in butt-welds

It has been well established, both theoretically and experimentally, that fatigue endurance decreases when plate thickness increases. Traditionally the thickness effect has been used so that the fatigue strength is reduced after a certain thickness limit upwards, usually 25 mm according to the following expression [1,14]:

$$\Delta\sigma_t = \Delta\sigma_{t_0} \left(\frac{t_0}{t}\right)^n \quad (9)$$

where $\Delta\sigma_t$ is the fatigue strength for a thickness t , $\Delta\sigma_{t_0}$ is the fatigue strength for the reference thickness, and n is based on test results. IIW-recommendation [1,14] suggests $t_0 = 25$ mm and $n = 0.25$ for butt-welds. Gurney [37] states that the current rule could be extrapolated back to thinner joints, but he also concludes that further work is needed to confirm the effect.

Fig. 5 shows estimated results of the fatigue endurance defined at 10^7 cycles as a function of the plate thickness for different initial

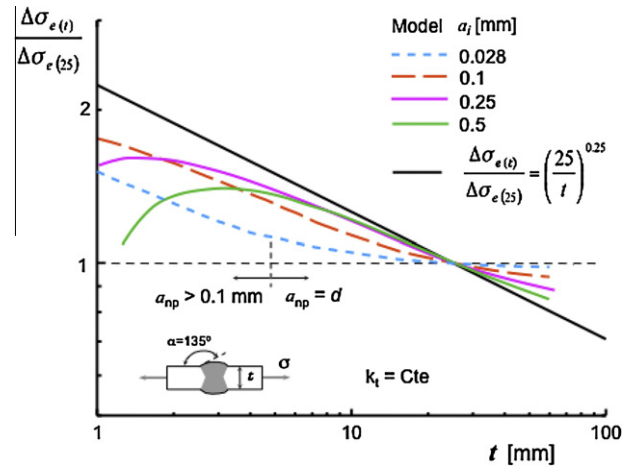


Fig. 5. Influence of plate thickness on fatigue strength of butt-welds (endurance: 10^7 cycles). Four different lengths a_i were considered.

crack lengths. Details and data can be obtained from Ref. [36]. The correction recommended by IIW for Expression (9) joints is also shown, extrapolated to thicknesses smaller than 25 mm. Even though the results show a general trend, i.e. the fatigue limit decreases with thickness as usually observed, notable differences in the influence of the initial crack length on the fatigue limit of thin plates are observed ($t < 10$ mm). In some cases the extrapolation of Expression (12) could overestimate the fatigue strength for thin plates. Estimated results show that an opposite trend could be found for thin plates ($t < 6$ mm) in the relation between fatigue limit and thickness when initial crack lengths are longer than about 0.3 mm. This opposite effect was observed experimentally by, for instance, Gustafsson [38] for non-load carrying attachments with 3 and 6 mm plate thickness.

In Fig. 5 the observed thickness effects are related with the effect of stress gradients and initial crack length. Another mechanism that can be part of thickness effect is the manufacturing or process history that can give rise to different grain and inclusion sizes and then different material fatigue properties. However, this effect is usually observed to be small when compared with gradient and initial crack length effects on fatigue strength. For initial crack lengths smaller than 0.1 mm, as the case of $a_i = 0.028$ mm, a smaller exponent appears from a given thickness (about 6 mm in Fig. 5). This is attributed to the fact that the influence of the stress gradient on fatigue limit decreases as the initial crack length decreases.

Fig. 6 shows four graphs with applied driving forces and the threshold for fatigue crack propagation, in terms of the stress intensity factor. Each graph corresponds to a given thickness: 1, 3, 6 and 25 mm, respectively. For each graph several applied driving forces are shown, given by the nominal stress level corresponding to the fatigue limit for the following initial crack lengths, a_i : 0.028 mm, 0.1 mm or 0.5 mm. It can be seen that below a given thickness, it is possible to obtain a non-propagating crack in the range of 0.08–0.18 mm. This is the reason for the different slope observed in Fig. 5 for $a_i = 0.028$ mm. In this case, the fatigue limit is given by $a_i = d = 0.028$ mm for a thickness greater than 6 mm, but it is given by a non-propagating crack of about 0.1 mm for a thickness smaller than 6 mm, and the slope of the relation becomes similar to the one for $a_i = 0.1$ mm. The relative position between the applied driving force distribution and the material crack propagation threshold curve seems to define a thickness range below which the fatigue limit is given by a non-propagating crack whose length ranges from 0.08 mm to 0.18 mm. As we will see later, these mechanisms could be the reason for the low scatter in fatigue strength experimentally observed for small reinforcement angles.

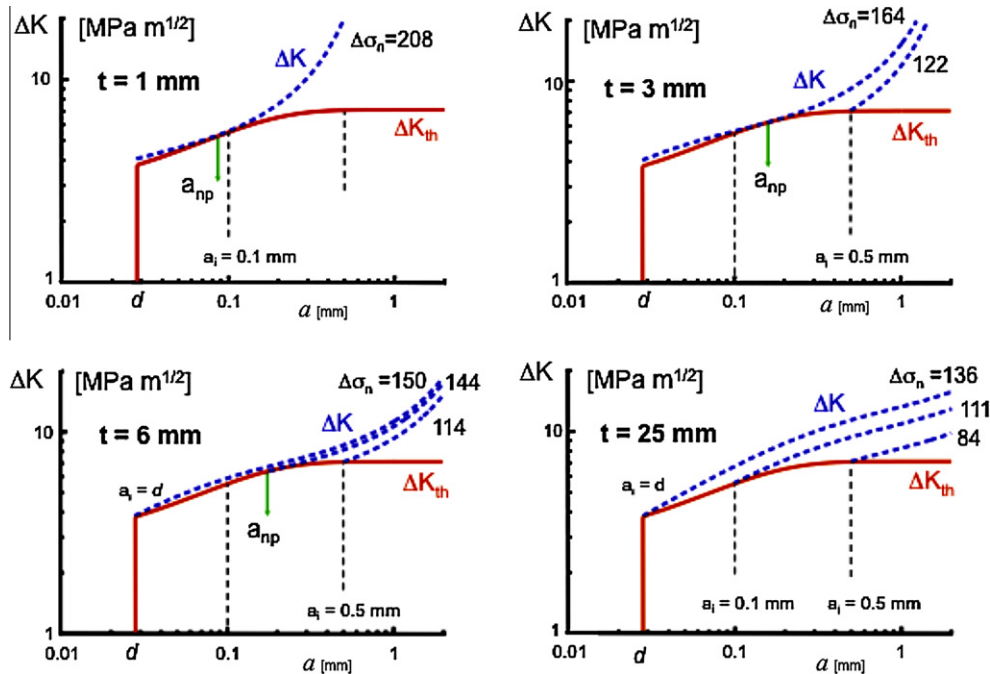


Fig. 6. Applied driving force (ΔK , dashed lines), and threshold for crack propagation (ΔK_{th} , bold lines), as a function of crack length for four different plate thicknesses: 1, 3, 6 and 25 mm. Nominal stresses ($\Delta\sigma_n$) for each ΔK curve correspond to the fatigue limit estimated for a given initial crack length ($a_i = d, 0.1$ mm or 0.5 mm).

4.2. Influence of reinforcement angle in butt-welds

Gurney [39] has pointed out that the range of values for the fatigue strength of butt welds varies widely, from 100 MPa to 180 MPa for R values close to zero. He points out that the main reason for these variations seems to be the local shape on the reinforcing cap, especially the angle α between the reinforcement and the base metal. Fig. 7 shows the well known experimental results presented by Gurney, together with results of the estimated fatigue limit as a function of the reinforcement angle for different initial crack lengths. Even though the estimated results seem to be a little lower than the experimental ones, the trend is well estimated. It is worth noting that the model can explain the reduction in the scatter observed as the reinforcement angle decreases. This is due to the fact that as the reinforcement angle decreases, the stress gradient near the weld toe increases and from a given value non-propagating cracks define the fatigue limit. Those non-propagating cracks are in the range of 0.1–0.2 mm, so that the fatigue limit would be similar for the cases of $a_i = 0.028, 0.1$ mm and 0.2 , as it can be observed for

$\alpha = 115^\circ$. The situation is similar to those shown in Fig. 6b and c, where it can be seen that the minimum applied nominal stress range ($\Delta\sigma_n$) for which a crack could propagate is almost not influenced by the initial crack length a_i , for $d < a_i < 0.18$ mm.

Fig. 7 also shows the results obtained with the material data corresponding to a bainite–martensite microstructure and an initial crack length $a_i = 0.05$ mm. It can be observed that the estimated curve falls above the upper limit of experimental results. The upper (B/M, $a_i = 0.05$ mm) and lower (F/P, $a_i = 0.5$ mm) estimated curves, which can be considered as an upper and lower limit, respectively, cover all experimental results. Estimations follow not only the trend in fatigue limit, which decreases as the reinforcement angle decreases, but also the trend of the scatter, which also decreases as the reinforcement angle decreases.

Because toe cracks usually nucleate at heat affected zones, where the microstructure has enhanced fatigue properties (bainite–martensite microstructure), estimations made by using ferrite–pearlite microstructure properties are usually conservative. For better estimations, the evolution of the fatigue properties could be also considered. The analysis of the definition of the microstructural parameter d for different steel microstructures and the influence of the development of the extrinsic component of the threshold, mainly defined by the parameter d and the smooth fatigue limit $\Delta\sigma_{eR}$, can be found in Refs. [28–31].

5. Theoretical and experimental analysis of butt-welded joints

In this section, we analyze the ability of the approach to estimate the fatigue crack propagation of small cracks propagating from a weld toe of a butt joint. To do so, a dedicated experimental methodology is implemented for the detection and monitoring of the development of surface small cracks initiated at weld toes.

5.1. Experiments

Butt welded joints with three different thicknesses ($1/4''$, $1/2''$ and $1''$) were prepared by using MIG welding. Joints were made of A36

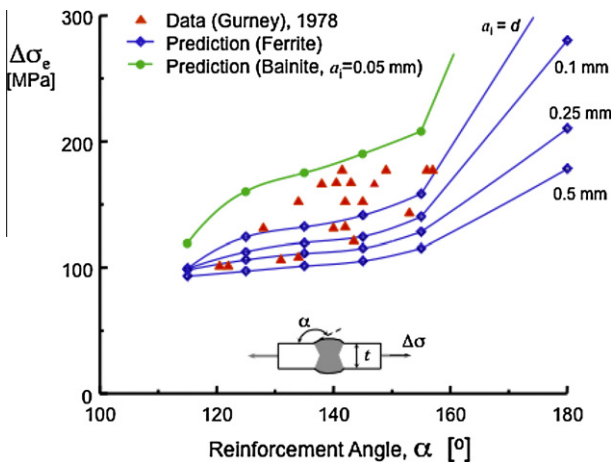


Fig. 7. Influence of reinforcement angle in fatigue strength of butt-welds.

grade steel with a yield stress of 250 MPa and a tensile strength of 475 MPa.

Specimens were prepared and fatigue tested by using a soft fatigue machine (Walking Beam type), with a configuration of four-point bending at a frequency of 10 Hz.

For the detection and monitoring of the development of surface small cracks, a multi-strain gauges technique was implemented. Fig. 8 shows photographs with details of specimens configuration and instrumentation with multiple strain gauges, which allowed to monitor the fatigue crack propagation from a crack length of 100 μm. Details of the method and the implementation can be found in Refs. [40–42].

5.2. Estimations

In order to apply the approach detailed in Section 3, it is necessary to measure the geometry of the joint, to estimate the applied ΔK as a function of crack length (by using finite element methods, weight function or other methodology), and to define the material parameter needed for the Expression (6) (ΔK_{th} vs. a). The applied driving force, ΔK, is related to the nominal stress range, Δσ_n, and crack length, a, by Expression (2), in which the parameter Y is a function of crack length, component geometry and type of loading. In this work, the estimation was carried out by using the superposition and the weight function methods and the following solution for a through thickness crack in a finite plate [42].

$$\Delta K = \frac{2}{\sqrt{\pi}} \int_0^a \left\{ \frac{\Delta \sigma_{yy}(x)}{\sqrt{a}} \left[\frac{3.52 \left(1 - \frac{x}{a}\right)}{\left(1 - \frac{a}{t}\right)^{3/2}} - \frac{4.35 - 5.28 \frac{x}{a}}{\left(1 - \frac{a}{t}\right)^{1/2}} \right] + \left(\frac{1.3 - 0.3 \left(\frac{x}{a}\right)^{3/2}}{\sqrt{1 - \left(\frac{x}{a}\right)^2}} + 0.83 - 1.76 \frac{x}{a} \right) \left(1 - \left(1 - \frac{x}{a}\right) \frac{a}{t}\right) \right\} dx \tag{10}$$

where *t* is the plate thickness and σ_{yy}(*x*) is the non-uniform stress field along the crack path. σ_{yy}(*x*) was estimated using finite element models constructed by using the ABAQUS code [43]. Eight-node quadratic elements were used in a static, elastic analysis.

For the as-welded joint the weld toe was modeled as a sharp corner, so that theoretical elastic stresses near the surface would tend to infinity. This is acceptable if crack-like initial defects exist almost continuously along the weld toe. Therefore, the stresses at the surface are not needed, but the stress from a depth equals to the considered initial crack length, whose value is usually greater than 0.1 mm. In a previous publication it was shown that the stress concentration obtained at different depths from the toe root, *k_{ts}*, does not depend on the notch root radius when *x* > 0.2ρ [36]. Because a value of 0.1 mm seems to be a reasonably minimum value to be considered as a minimum initial crack length for weld details, the influence of notch root radius seems to have no important effect in the applied stress distribution, unless the notch root radii are greater than 0.5 mm. A greater toe radius would give lower stress concentrations, so that in those cases the assumption would be conservative. If it is necessary, the toe radius could be easily included in the analysis by accounting for it when estimating the stress distribution by using finite element models.

Fatigue properties of a C–Mn steel with ferrite–pearlite microstructure were used conservatively. Microstructural dimension, plain fatigue limit and threshold for long crack were experimentally measured according to standards [44,45] (see Table 1). The propagation threshold as a function of crack length in terms of the stress intensity factor range (ΔK_{th} vs. a) or the threshold stress (Δσ_{th} vs. a), was estimated by using Expressions (6), (7) and (8). Estimations were made with applied *R* = 0.1, residual stress of about half the yield stress (so that the effective load ratio was considered to be about 0.4), final crack length *a_f* = *t*/2, *t* = 12.5 mm, and *d* = 0.028 mm (average ferrite grain size).

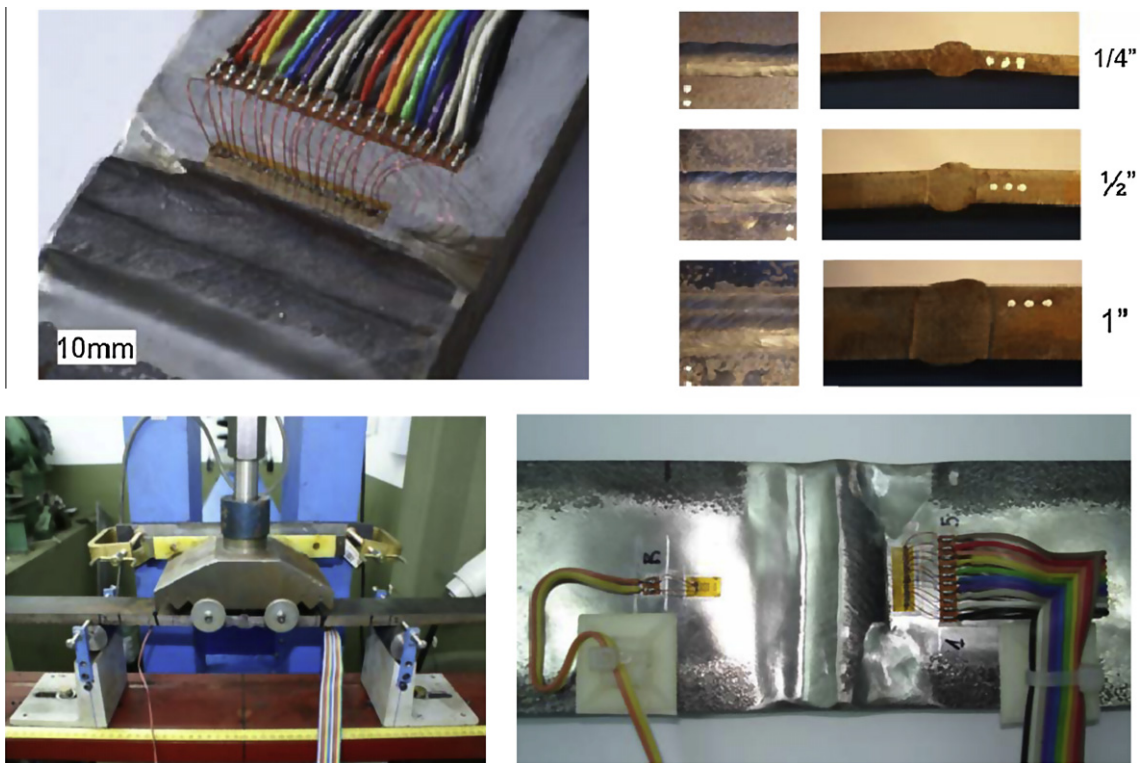


Fig. 8. Photographs showing details of the instrumented specimens and testing configuration.

Table 1
Material chemical composition and mechanical properties used for the application in Section 5.

C–Mn Steel						
Ferrite–Pearlite (F/P) microstructure						
0.11 wt.% C 0.38 wt.% Mn 0.2 wt.% Si 0.013 wt.% P 0.018 wt.% S						
σ_{ys} (MPa)	σ_u (MPa)	d (mm)	$\Delta\sigma_e R = 0.1$ (MPa)	ΔK_{thr} (MPa m ^{1/2})	C (mm/cycle)	m
286	472	0.028	360	7.6–5.7 R	1.526×10^{-9}	3.15

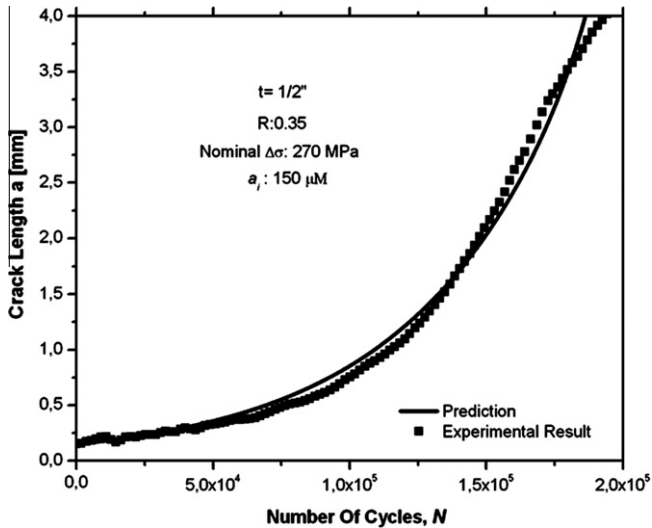


Fig. 9. Example of the experimental measured and predicted fatigue crack lengths as a function of number of cycles for a butt welded joint.

The basic concept used in this work is that the effective driving force applied to the crack is given by the difference between the total applied driving force, defined by the applied stress intensity factor range for a given geometrical and loading configuration, ΔK , and the threshold for crack propagation as a function of crack length, ΔK_{th} (see Fig. 3). ΔK and ΔK_{th} are estimated using Expression (10) and (6), respectively. Finally, the fatigue crack propagation life is estimated integrating Expression (5) for a given crack length range. The initial crack length a_i is defined by the greater defect present at the weld toe. Failure was assumed to occur at a final crack length, a_f , defined as half the plate thickness.

5.3. Results and discussions

Fig. 9 shows an example of the results of monitoring the fatigue propagation of a crack initiated from a weld toe. It can be observed that the method has a detection threshold of about 100–200 μm , which also allows to monitor the crack propagation during the early stage of fatigue. Good agreement is observed in the total crack range, mainly for crack lengths smaller than 1 mm. It can also be observed that the number of cycles necessary to propagate the crack length from 0.1 mm to 1 mm was about 60% of the total monitored fatigue crack propagation life.

Fig. 10 shows the experimental results and the estimated fatigue lives for butt joints with three different thicknesses. Initial crack length was chosen as $a_i = 0.150$ mm. As we have mentioned in the introduction, a review by Grover [8] suggested that even high-quality welds contain flaws up to a depth of about 0.1 mm, that other previous works on fatigue of welded joint have observed initial crack-like defect depths of about 10–400 μm [9–11] according to the welding conditions and applied quality control, and that Radaj and Sonsino have recommended initial crack size $a_i = 0.1$ –0.25 mm in welded structures for life predictions [2]. An

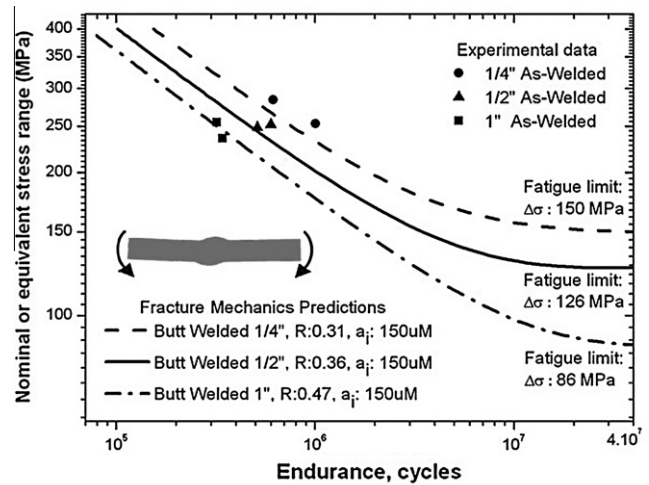


Fig. 10. Experimental and predicted fatigue lives for butt joints.

initial defect size of about 150 μm seems to be a proper estimation for good quality welds. Besides, this value is similar to the detection threshold of the experimental technique used to detect and monitor the crack evolution, so that comparisons of estimated and experimental results could be done.

Even though the tests were carried out at relatively high nominal stresses, the estimations show a good correlation and trends. It can also be seen in Fig. 10 that the approach allows to obtain an associated fatigue limit for any analyzed configuration, and that the estimation of the fatigue limit for 1" thickness is in good correlation with the value given by IIW FAT curve (80 MPa for this case) [1,14].

6. Estimation of the fatigue threshold for a non-load-carrying transverse fillet welded joints

Results, conclusions and suggestions of an interesting paper recently published by Zhang and Maddox [46] are analyzed in order to show how important the proposed approach is to study and understand the influence of the different parameters on the fatigue behavior of welded joints. Zhang and Maddox have presented the results of an investigation of the effect of weld toe burr grinding on the fatigue performance of non-load-carrying transverse fillet welded joints. In that work, both experiments and calculations based on fracture mechanics suggest that the fatigue lives of the toe ground joints in short life regime ($<10^6$ cycles) were dominated by the crack propagation process, while in the long life regime ($>10^6$ cycles) crack initiation became significant. Reasonable estimates of the crack initiation period were made using the local stress approach proposed by Lawrence et al. [47]. The investigation also suggested that more benefits from weld toe grinding could be claimed in the long ($N > 10^6$ cycles) than the short life regime (by a factor of at least 4.6 in that work). When compared with as-welded joints, the increased fatigue performance of ground joints was

attributed to reduced stress intensity magnification factor M_k , reduced ΔK due to more favorable fatigue crack front shapes, and slower crack growth rates possibly related to reduced tensile residual stresses.

Fig. 11 shows the experimental results obtained by Zhang and Maddox for as-welded and toe grounded welds, including the mean S–N curve reported by Booth [48] for burr ground joints. Experimental results proved to be in good agreement with the BS 7608. Class F mean curve, the appropriate class for as-welded joints of this type [49], is also shown. Fig. 11 also shows the estimated fatigue life carried out by Zhang and Maddox. The fatigue performance of all the ground joints was significantly better than that of the as-welded joints. The life increase factor (LIF), defined as the ratio of the fatigue endurance of ground welds to that of the as-welded joints (assumed to correspond to the Class F mean curve), ranged from 4.6 to 18.4, with an average value of 7.4, at least double the design factor of 2.2 recommended in BS 7608 for ground welds (corresponding to a 30% increase in the allowed stress range). An important result is related with one specimen that was tested at a stress range of 180 MPa. After 5.46×10^6 cycles, which exceeded 18 times the fatigue life for the Class F mean curve, there was still no indication of fatigue crack initiation, and the result was treated as a run-out.

According to the results and analysis made by Zhang and Maddox for both cases (as-welded and ground joints), the following two descriptions can be summarized. For the case of the as-welded joint, for which an initial crack length of 0.15 mm is assumed, the fatigue life (or fatigue resistance) is calculated by integrating the fracture mechanics-based fatigue crack growth law of Expression (1) for the material comprised between the limits of flaw size and critical crack size corresponding to failure [50,51]. The initial crack length (0.15 mm) is clearly inside the short crack regime, so that the short crack effect is not considered in the approach. By assuming the exponent $m = 3.0$, the average value of parameter C was determined to be 1.3×10^{-13} by using the experimental results and fatigue crack propagation rate data obtained from beach marks [47]. Calculations were made using the 3D M_k solution for as-welded joints [18]. The estimated fatigue endurance, based on fatigue crack growth only, agreed well with their experimental data, which, except for the test results from specimens beyond 10^6 cycles, fall between the two estimates for the different initial flaw sizes assumed (0.15 and 0.2 mm). Good results for the estimations are clearly expected because an average value of the parameter A for Expression (1) is estimated by using the same experimental results. The initial crack length (0.15 mm) is clearly inside the short crack regime, as mentioned before, so that the short crack effect is not considered in the approach.

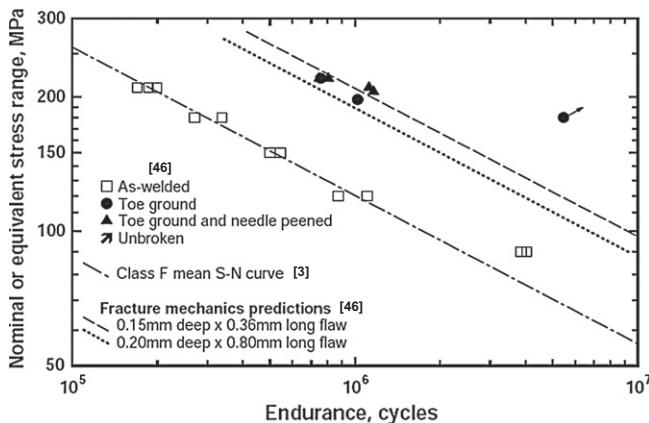


Fig. 11. Experimental and estimated results reported by Zhang and Maddox for as-welded and toe grounded non-load-carrying transverse fillet welded joints [46].

On the other hand, for the case of the ground joint, a fatigue crack initiation life was contemplated and calculated by using a local approach developed by Morrow [52], as part of the evaluation of the total fatigue strength of welded joints. This was defined as the number of cycles required to create a crack of a certain size. It was estimated using a low-cycle fatigue (LCF) approach which utilized a Coffin–Manson type equation. The LCF properties of the heat affected zone (HAZ), where crack initiation occurred, were estimated by applying the empirical relation between hardness and tensile strength of steels. The percentage of the total life spent initiating a crack was predicted to increase with increasing fatigue endurance. A weakness in the approach is that the transition crack size, at which the fatigue damage process is assumed to change from crack initiation to crack growth, has been defined arbitrarily, ranging from 0.1 mm [53], to 0.15 mm [54] to 0.25 mm [46]. The authors also addressed that the assumption that part of the fatigue life of a welded joint is governed by the tensile strength of the material is in direct contradiction of the well established finding that the fatigue lives of welded joints are independent of the material's tensile strength. They also addressed that this is one of the reasons why the approach is not generally used to assess as-welded joints. However, the approach proposed in the present paper (see Section 3) can clearly account for the influence of the material properties on the definition of the fatigue strength of the weld, and states how that influence can be minimized by the more important initial crack-like defect size influence and the statistical nature of the phenomenon. Fatigue test results are usually presented as $\Delta\sigma_n$ – N curves where the different levels are hidden by the variation in fatigue strength due to the main influence of initial crack length and residual stresses. These effects can be clearly observed in the analysis of Section 4. To uncover the relevant differences, statistical methods are needed.

Fig. 12 shows the fatigue lives estimated for both joints (as-welded and ground joints) by using the integrated fracture mechanic approach (IFMA) described in Section 3. Procedure was similar to that described in Section 4 for butt joint. Fig. 12 also shows details of the two FE models used for calculations of $\Delta\sigma_{yy}(x)$. Estimation were made with applied $R = 0.1$, residual stress of about half the yield stress (so that the effective load ratio was considered to be about 0.4), final crack length $a_f = t/2$, $d = 0.02$ mm (average ferrite grain size), and $a_i = 0.2$ mm and 0.04 mm for as-welded and ground joints respectively. Most data were obtained from Ref. [46]. Initial crack length was chosen as $a_i = 0.2$ mm for the as-welded joint and as $a_i = 0.04$ mm for the ground joint, according to the analysis of the initial defect sizes given in Ref. [46]. Fig. 12 shows that the estimated results agree very well with experimental results. It is worth noting that estimations are made without the need of experiments with the weld joints. The approach needs the geometry and some weld conditions of the joint, some material parameters and the evaluations of the maximum initial defect size. It is also worth noting that the approach allows the estimation of the fatigue limit associated to the weld joint.

Fig. 12 also shows that the actual lives are greater than the ones estimated by Zhang and Maddox for longer endurance ($>10^6$). Those authors suggested that there is a significant fatigue crack initiation phase in the fatigue life, and that by ignoring it the fatigue endurance of ground joints is underestimated. However, it can be seen that the difference is due to the inability of the used approach to define a fatigue limit (associated threshold for fatigue crack propagation). If Expression (5) is used instead of 1, and the threshold can be estimated as a function of crack length, a given threshold for the weld joint can be obtained. Results clearly show that the proposed approach detailed in Section 3 of this paper can properly estimate the improvement in fatigue strength due to grinding, without invoking any fatigue crack initiation stage. Since the main purpose of the grinding process is to eliminate initial defects at the

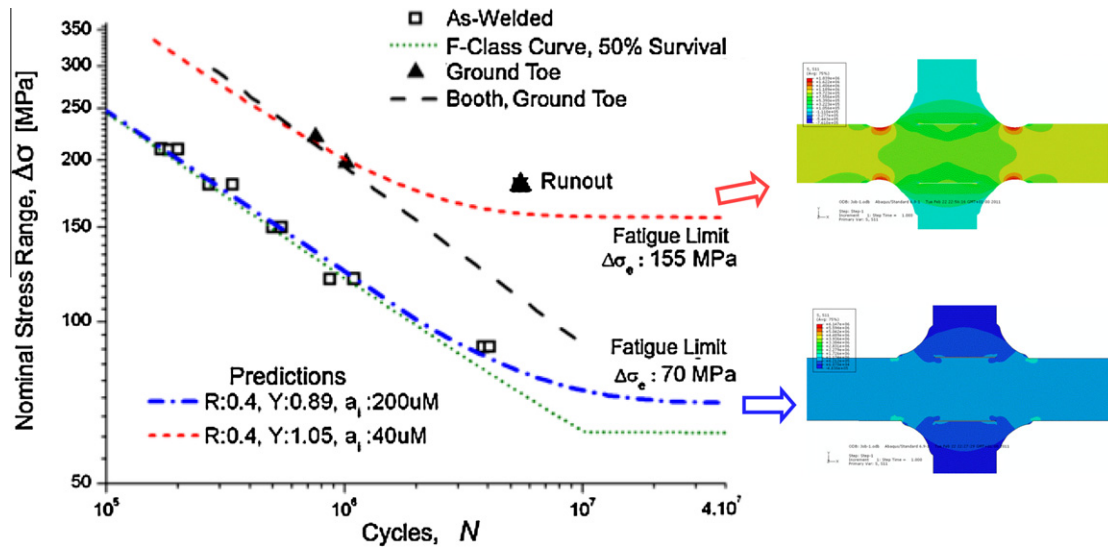


Fig. 12. Experimental [46] results reported by Zhang and Maddox for as-welded and toe grounded non-load-carrying transverse fillet welded joints, and results predicted by using the approach detailed in Section 3.

weld toe, this effect can be taken into account in the proposed approach by reducing the initial crack length to a minimum value ($a_i = 0.04$ mm).

Although it may be arguable whether crack initiation life is significant or not for as-welded joints, it is generally believed that one of the main benefits of toe grinding is to remove welding-induced flaws, which should significantly increase the crack initiation endurance and hence the total fatigue life. However, the work by Zhang and Maddox suggested that crack initiation quickly took place from flaws on or just below the ground surface when the applied stress ranges were above a certain stress level. Although the probability of crack initiation from a flaw was reduced in ground joints, their analysis clearly demonstrated that the majority of the fatigue cracks (a total of eleven) initiated at flaws. However, their sizes were smaller than those observed in the as-welded joint (about 0.040 mm, against 0.2 mm in the as-welded condition). This was consistent with the observation that these cracks initiated in weld metal, not in the parent metal where the SCF due to the groove produced by grinding was the highest for the ground joints.

Zhang and Maddox indicated that the beneficial effects of toe grinding can be attributed to the following two aspects. A reduced stress intensity factor range, ΔK , when compared at the same nominal stress range and crack size, attributed to the reduced stress intensity magnification factor M_k and a lower crack aspect ratio. And secondly, a lower crack growth rate that can be explained by the possible difference in residual stresses. The reduction of the applied ΔK due to the change in geometry introduced by grinding can be accounted in the proposed approach. However, the threshold condition that defines the fatigue limit associated to the ground joint is not influenced by the propagation properties, as it can be observed schematically in Fig. 4. The other important factor that changes the fatigue strength is the shorter initial crack length, given by the shorter crack-like defects present in the ground joint when compared with the as-welded one.

Of course, and it is clear from the results, much effort should be made to avoid defects or grind them out. The fatigue limit and, above all, fatigue life can be improved by adding a significant crack initiation period required before a fatigue crack starts to propagate. However, the maximum fatigue limit that could be possible for a given set of geometry and material and residual stress distributions is clearly given by the threshold condition defined by the threshold curve ΔK_{th} (given for instance by Expression (6)) and

the applied curve ΔK (see Fig. 4), both as a function of the crack length.

7. Concluding remarks

This work stresses the importance of considering the fatigue threshold condition and the short crack effect in the definition of fatigue strength and behavior of welded joints. The proposed integrated fracture mechanics approach (IFMA) has shown to be able to describe the influence of most of the parameters and their interactions involved and to provide a powerful tool to estimate the fatigue strength of different weld configurations, including those where short crack propagation should be considered.

By making use of advanced meshing techniques and sub-modeling, it is now possible to have information on local stresses near a feature of interest. On the other hand, some aspects of welded joints remain difficult to model accurately. Local residual stresses and variation in material properties across the weld are two other features which are, and will remain for some time, beyond the capabilities of the design engineer to model accurately. However, it is of great importance to be able to quantify the influence of each parameter involved in the definition of the fatigue behavior of a given weld joint configuration. Once the approach is available, many trend and limitations can be properly estimated. The possibility of measuring all the necessary parameters will then improve even more the ability of the approach to estimate the fatigue behavior. Conservative simplifications are also possible.

Today, the fracture mechanics approach is well established particularly for the fatigue assessment of welded joints and offers the one and only way for fitness for purpose assessment of structural members with flaws or other crack-like defects. The analysis presented in this paper shows that the proposed approach can also be used for design and results clearly show its ability to predict the effect of scaling, defect size, micro and macrogeometry (and change in geometry), residual stresses, material properties, etc. Authors believe that much effort should be spent in this direction.

Acknowledgements

Authors wish to express their gratitude to the funding provided by CONICET (Consejo Nacional de Investigaciones Científicas y

Técnicas), and by Agencia Nacional de Promoción Científica y Tecnológica, Argentina (PICT2010 No. 0379), and to the weld joints provided by Fundación Latinoamericana de Soldadura (FLS) and ESAB Argentina.

References

- [1] Hobbacher A, editor. Recommendations for fatigue design of welded joints and components. IIV Doc XIII-2151r1-07/XV-1254r1-07. Int Inst Welding; 2007.
- [2] Radaj D, Sonsino CM, Fricke W. Fatigue assessment of welded joints by local approaches. 2nd ed. Cambridge: Woodhead Publishing and Boca Raton Fla: CRC Press; 2006.
- [3] Radaj D. Review of fatigue strength assessment of nonwelded and welded structures based on local parameters. Int J Fatigue 1996;18:153–70.
- [4] Sonsino CM, Kassner M. Übersicht über Konzepte zur schwingfesten Bemessung von Schweißverbindungen. Report 236. Düsseldorf: DVS-Verlag; 2005. p. 12–23.
- [5] Maddox SJ. Fatigue strength of welded structures. 2nd ed. Abington Publishing; 1991.
- [6] Signes EG, Baker RG, Harrison JD, Burdekin FM. Factors affecting the fatigue strength of welded high strength steels. Br Weld J 1967;14:108–16.
- [7] Lopez LM, Korsgren P. Characterization of initial defect distribution and weld geometry in welded fatigue test specimens. In: Blom AF, editor. Proc of the fatigue under spectrum loading and in corrosion environments. EMAS; 1993. p. 3–21.
- [8] Grover JL. Initial flaw size estimating procedures for fatigue crack growth calculations. In: Maddox SJ, editor. Proc of the international conference on fatigue of welded construction. Brighton; 1987. p. 275–85.
- [9] Smith IFC, Smith RA. Fatigue Fract Eng Mater Struct 1982;5(2):151–65.
- [10] Signes EG, Baker RG, Harrison HD, Burdekin FM. Weld J 1967;14:108–16.
- [11] Watkinson F, Bodger PH, Harrison JD. The fatigue strength of welded joints in high strength steels and methods for its improvement. In: Proceedings of the conference on fatigue of welded structures. The Welding Institute. Brighton; 1970. p. 97–113.
- [12] Verreman Y, Nie B. Fatigue Fract Eng Mater Struct 1996;19:669–81.
- [13] Anderson TL. Fracture mechanics. 2nd ed. Boca Raton, Florida: CRC Press, Inc.; 1995.
- [14] Hobbacher A. A fatigue design of welded joints and components. International Institute of Welding. Doc. XIII-1539-96; 1996.
- [15] BS 7608. Fatigue design and assessment of steel structures – code of practice. London: British Standards Institution; 1993.
- [16] BS 7910. Guide on methods for assessing the acceptability of flaws in metallic structures. London: British Standards Institution; 1999.
- [17] Guideline for fatigue design of steel constructions: Japan Society of Steel Construction (JSSC). Tokyo, (Japan): Gihodo Ltd.; 1993.
- [18] BS 7910. Guide on methods for assessing the acceptability of flaws in metallic structures (Incorporating Amendment 1). London: British Standards Institution; 2005.
- [19] Smith IFC, Smith RA. Eng Fract Mech 1983;18(4):861–9.
- [20] Lawrence FV. Welding Research 1973;52(Suppl.):212s–20s.
- [21] Nguyen NT, Wahab MA. Eng Fract Mech 1996;55(3):453–69.
- [22] Lie ST, Lan S. Int J Fatigue 1998;20(6):433–9.
- [23] Haagensen PJ. IIV's round robin and design recommendations for improvement methods. In: Maddox SJ, Prager M, editors. Proc of international conference on performance of dynamically loaded welded structures, IIV 50th Annual Assembly Conference. 1997. p. 305–16.
- [24] Santus C, Taylor D. Physically short crack propagation in metals during high cycle fatigue. Int J Fatigue 2009;31:1356–65.
- [25] Chan KS, Lankford J, Davidson DL. J Eng Mater Technol 1986;108:20–36.
- [26] Suresh S, Ritchie RO. Int Met Rev 1984;29:445–75.
- [27] Miller KJ, de los Rios ER. The behaviour of short fatigue cracks. London: EGF Publication; 1988.
- [28] Chapetti MD, Kitano T, Tagawa T, Miyata T. Fatigue Fract Eng Mater Struct 1998;21:1525–36.
- [29] Chapetti MD, Kitano T, Tagawa T, Miyata T. Fatigue limit of blunt-notched components. Fatigue Fract Eng Mater Struct 1998;21(1998):1525–36.
- [30] Chapetti MD, Kitano T, Tagawa T, Miyata T. Two small-crack extension force concept applied to fatigue limit of blunt notched components. Int J Fatigue 1999;21(1):77–82.
- [31] Chapetti MD. Fatigue propagation threshold of short cracks under constant amplitude loading. Int J Fatigue 2003;25(12):1319–26.
- [32] McEvily AJ, Minakawa K. Eng Fract Mech 1987;28(5–6):519–27.
- [33] El Haddad MH, Topper TH, Smith KN. Eng Fract Mech 1979;11:573–84.
- [34] Tanaka K, Akiniwa Y. Eng Fract Mech 1988;30(6):863–76.
- [35] Miller KJ. Fatigue Fract Eng Mater Struct 1993;16(9):931–9.
- [36] Chapetti MD, Belmonte J, Tagawa T, Miyata T. An integrated fracture mechanics approach to analyze the fatigue behaviour of welded joints. J Sci Technol Weld Joi 2004;9(5):430–9.
- [37] Gurney TR. Fatigue of thin walled joint under complex loading. Cambridge, (UK): Abington Publishing; 1997.
- [38] Gustafsson M. Thickness effect in fatigue of welded extra high strength steel joints design and analysis of welded high strength steel structures. West Midlands: EMAS Ltd.; 2002. p. 205–24.
- [39] Gurney TA. Fatigue welded structures. Cambridge, (UK): Cambridge University Press; 1978.
- [40] Chapetti MD, Otegui JL. Controlled toe waviness as a means to increase fatigue resistance of automatic welds in transverse loading. Int J Fatigue 1997;19(10):667–75.
- [41] Chapetti MD, Otegui JL. Importance of toe irregularity on fatigue resistance of automatic welds. Int J Fatigue 1995;17(8):531–8.
- [42] Murakami Y. Stress intensity factors handbook. The society of materials science. Oxford, (England): Pergamon Press; 1987.
- [43] Abaqus® User Manual. Dassault Systèmes; 2007.
- [44] ASTM E 466-96. Standart Practice for conducting force controlled constant amplitude axial fatigue test of metallic materials, vol. 03.01. PA: Annual Book of American Society for Testing and Materials Standards; 2001.
- [45] ASTM E 647-00. Standart test for measurement of fatigue crack growth rates, vol. 03.01. PA: Annual Book of American Society for Testing and Materials Standards; 2001.
- [46] Zhang YH, Maddox SJ. Fatigue life prediction for toe ground welded joints. Int J Fatigue 2009;31:1124–36.
- [47] Lawrence FV, Mattos RJ, Higashida Y, Burk JD. Estimating the fatigue crack initiation life of welds. In: Hoepfner DW, editor. Fatigue testing of weldments. ASTM STP 648. American Society for Testing and Materials; 1978. p. 134–58.
- [48] Booth GS. Improving the fatigue strength of welded joints by grinding techniques and benefits. Met Constr 1986;18(7):432–7.
- [49] BS 7608. Fatigue design and assessment of steel structures. London: British Standards Institution; 1993.
- [50] Maddox SJ. A fracture mechanics analysis of the fatigue strength of welded joints. PhD thesis. University of London; 1972.
- [51] Samuelson J, Dahlberg L. Fracture mechanics design of welded joints: review and practical applications. In: Maddox SJ, editor. Proc of the international conference on fatigue of welded construction. Brighton; 1987. p. 265–74.
- [52] Morrow J. SAE Fatigue design handbook. In: Graham F, editor. 1968. p. 21–30.
- [53] Lassen T, Recho N. Fatigue life analysis of welded structures. ISTE Ltd.; 2006.
- [54] Moura-Branco CA, Gomes EC. Development of fatigue design curves for weld improved joints. In: Marquis G, Solin J, editors. Fatigue design 1995, vol. III. Finland: Helsinki; 1995. p. 9–20 [VIT Symposium 157].